

Mechanical and Morphological Analysis of 3D-Printed Polylactic Acid-Polybutylene Adipate Terephthalate Composite

Suchetha N. Raju^{1,*}, S.H. Kameshwari Devi¹, K.P. Ajeya² and K. Prashantha²

¹Department of Polymer Science and Technology, Sri Jayachamarajendra College of Engineering JSS Science and Technology University, Mysure – 570006, India

²ACU-Centre for Research and Innovation, Adichunchanagiri School of Natural Sciences, Adichunchanagiri University, B.G. Nagara, Mandya District-571448, Karnataka, India

Abstract: In this research paper, a detailed examination of the mechanical properties and morphologies of PLA and PBAT polymer blend materials which were produced through 3D printing techniques was conducted. The examination was completed using a PLA/PBAT/Joncryl blended material with a composition ratio of 77/20/3 wt% and manufactured through FDM techniques and an experimental design technique known as the Taguchi method to evaluate the effects of various manufacturing parameters on the mechanical characteristics of the material. This study investigates the mechanical and morphological performance of FDM-printed PLA/PBAT/Joncryl blend specimens using a Taguchi L9 design. A PLA/PBAT/Joncryl blend (77/20/3 wt%) was fabricated and printed by varying layer height (0.16–0.24 mm), printing temperature (190–210 °C), and infill density (50–100%). The optimal condition (0.16 mm, 210 °C, 100% infill) produced a maximum tensile strength of 41.20 N/mm² and elongation of 12.42%. ANOVA results confirmed infill density as the most significant parameter contributing 81.35% of the variance (P = 0.009). SEM revealed reduced voids and improved interlayer fusion at higher infill levels, while DMA showed higher storage modulus (~2200 MPa) for 100% infill specimens. The findings provide a process–structure–property relationship for optimizing biodegradable PLA/PBAT components for high-strength applications. This study illustrates that the infill % is the primary parameter that should be adjusted, while the layer height and printing temperature contribute but to a lesser extent to the improved performance of biodegradable PLA/PBAT/Joncryl blends.

Keywords: Polylactic Acid, Polybutylene Adipate Terephthalate, Polymer blends, Fused Deposition Modeling, Infill density, Mechanical properties, Dynamic Mechanical Analysis, Scanning Electron Microscopy, Biodegradable polymers, Additive Manufacturing.

1. INTRODUCTION

Additive manufacturing (AM) is a significant technological change that makes it possible to quickly produce the components that are custom, made, have complex geometries, use very little material, and have short lead times in comparison to the traditional manufacturing methods [1, 2]. FDM (Fused Deposition Modeling) is one of the AM methods that has attracted attention owing to its relatively low cost, ability to use a wide variety of thermoplastics, and simplicity of operation [3]. Biodegradable polymers, as a source of raw materials for 3D printing, have been the focus of researchers' interest in the last couple of years, especially in the fields of biomedical engineering, packaging, and products that are environmentally friendly [4, 5]. Polylactic acid (PLA) is a polymer that has widely been used in FDM as a biodegradable material mainly because of its good stiffness, dimensional accuracy, and biobased origin [6]. However, the problem with PLA is that it is a brittle type of plastic, having low impact resistance and limited thermal stability, thus it is hardly ever mixed with load, bearing and dynamically stressed components [7, 8]. As a result, scientists have started mixing ductile polymers with PLA in a solvent in order to increase the flexibility, toughness, and thermal performance [9].

Polybutylene adipate co-terephthalate (PBAT) is biodegradable aliphatic–aromatic co-polyester characterized by its high ductility, flexibility, and biodegradability [10, 11]. Blending PLA with PBAT has been reported to improve elongation at break, impact resistance, and overall toughness, though it often results in decreased tensile strength and stiffness due to the immiscibility of the two polymers [12, 13]. Several studies have examined compatibilizers, blend ratios, and processing conditions to optimize the balance between strength and ductility in PLA/PBAT blends [14, 15]. A reactive compatibilizer was incorporated in this study to enhance the compatibility and mechanical performance of PLA/PBAT/ *Joncryl* blends during FDM processing. The compatibilizer promotes interfacial adhesion by reducing phase separation and improving stress transfer between the PLA-rich and PBAT-rich phases, thereby contributing to improved strength and ductility. Moreover, reactive compatibilization assists in refining the blend morphology and reducing interlayer defects formed during extrusion and printing. The use of compatibilizer was therefore adopted to obtain a stable PLA/PBAT/ *Joncryl* composite filament with improved printability and balanced mechanical response. Parameters of the process such as infill pattern, infill density, printing speed, fan speed, printing and bed temperature have an essential role in defining the mechanical and thermal properties of PLA/PBAT blends for 3D printing [16, 17]. The paper has asserted that the optimal

*Address correspondence to this author at the Department of Polymer Science and Technology, Sri Jayachamarajendra College of Engineering JSS Science and Technology University, Mysure – 570006, India; E-mail: suchetha@sjce.ac.in

printing conditions might have a revolutionary effect on the crystallinity, interfacial bonding, and morphological features of polymer blends [18]. Besides that, the detailed surface examination by Scanning Electron Microscope (SEM) has revealed that the main factors determining the fracture mechanisms, thus the durability of FDM, printed parts, are phase separation, and interfacial adhesion, which is also confirmed by reference [19]. The investigation of viscoelastic behavior in PLA/PBAT/Joncryl blends by means of Dynamic Mechanical Analysis (DMA) has been accomplished [20]. The objective of the proposed research work is to provide a comprehensive and scientific examination of the mechanical, thermal, and morphological characteristics of the PLA/PBAT/Joncryl materials used to produce 3D prints through the Additive Manufacturing process, Fused Deposition Modeling (FDM). Tensile testing, DMA analysis, and SEM will be conducted to examine the impact of varying layer thickness, temperatures, and densities on the tensile strength properties, and the impact of layer thickness on the thermal properties. The novelty in this study is emphasized through the integration of Taguchi optimization with mechanical testing, ANOVA-based parameter ranking, SEM fracture morphology, and DMA-based thermo-mechanical analysis.

2. EXPERIMENTAL INVESTIGATION

2.1. Materials

Commercial-grade PLA, PBAT and Joncryl pellets granules were obtained from Bio green Biotech-Bangalore, with all the materials meeting standard specifications for 3D printing and polymer blending. Prior to processing, PLA, PBAT and Joncryl were dried in a vacuum oven at 50 °C and 60 °C respectively for 6 hours to eliminate moisture and prevent hydrolytic degradation during extrusion.

2.2. Preparation of PLA/PBAT Blends

PLA, PBAT, Joncryl were melt-blended in a weight ratio of 77/20/3 (PLA/PBAT/Joncryl) using a co-rotating twin-screw extruder (Process 11, Thermo Scientific, Thermo Fisher Scientific, Germany). Joncryl was incorporated as a reactive compatibilizer to overcome the inherent immiscibility between PLA and PBAT, which otherwise leads to poor interfacial adhesion,

phase separation, and inferior mechanical properties. The epoxy-functional groups of Joncryl react with the terminal hydroxyl and carboxyl groups of both polymers during melt processing, resulting in chain extension, improved interfacial bonding, refined morphology, and enhanced mechanical performance. Extrusion was carried out under a controlled temperature profile across the barrel zones: 160 ± 5 °C (Zone 1), 170 ± 5 °C (Zone 2), 180 ± 5 °C (Zone 3), and 190 ± 5 °C at the die zone, with a screw speed of 60 rpm. The homogeneous extrudate strands were air-cooled, pelletized, and subsequently oven-dried at 50 °C for 4 h to eliminate residual moisture. The dried blend pellets were converted into filaments of 1.75 ± 0.05 mm diameter with a single, screw filament extruder (Model: Noztek Pro, Noztek Ltd., UK). The barrel temperature zones during filament extrusion were 165 °C (feed zone), 175 °C (compression zone), and 185 °C (die zone) with a screw speed of 25 rpm and nozzle diameter of 2 mm. The extruded filaments were cooled in air and spun under controlled tension to obtain uniform diameter and smooth surface finish, thus, making them suitable for Fused Deposition Modelling (FDM) printing applications.

2.3. Experimental Design and Parameter Justification

A Taguchi Design of Experiments (DoE) methodology was employed to systematically evaluate the effects of key process variables on the mechanical and thermal performance of PLA/PBAT/Joncryl (77/20/3) 3D-printed parts. The following three control factors were considered:

A – Layer Height	: 0.16, 0.20, 0.24
B – Printing Temperature (°C)	: 190, 200, 210
C – Infill density (%)	: 50%, 75%, 100%

An L9 orthogonal array was selected to efficiently minimize the number of experimental runs while maintaining a balanced design for statistical analysis. The response variables measured included tensile strength, elongation at break. Signal-to-noise (S/N) ratios were calculated for each response to identify optimal levels. In the Taguchi method, the signal-to-noise (S/N) ratio is a way to measure

Table 1: Printing Parameters Level Setting of PLA/PBAT/ Joncryl Composite

Level	Layer Height - LH (mm)	Printing Temp -PT (°C)	Infill Density - ID (%)
L1	0.16	190	50
L2	0.20	200	75
L3	0.24	210	100

Table 2: Experimental Design Matrix Showing Selected Process Parameter Combinations of Layer Height (LH), Printing Temperature (PT), and Infill Density (ID) for FDM Trials

Trails	Layer Height - LH (mm)	Printing Temp -PT (°C)	Infill Density - ID (%)
1	0.16	190	50
2	0.16	200	75
3	0.16	210	100
4	0.2	200	100
5	0.2	210	50
6	0.2	190	75
7	0.24	210	75
8	0.24	190	100
9	0.24	200	50

performance robustness — how well a process achieves a desired outcome despite variability (“noise”). The “higher-the-better” concept is one of the three common S/N formulations used, and it’s applied when the goal is to maximize the response value.

Layer height is the thickness of each layer that is deposited during Fused Deposition Modeling (FDM). The printing pattern was set to a rectilinear (0/90 alternating raster) infill orientation in this study, which offers a good balance of strength and dimensional stability. The printing speed was kept at 50 mm/s to allow for a steady material flow and good inter, layer adhesion. Smaller layer heights (e. g., 0.16 mm) were chosen to get a better surface finish and higher mechanical strength due to stronger inter, layer fusion, although the printing time is longer. On the other hand, bigger layer heights (e. g., 0.24 mm) were chosen for quicker printing, but with a loss in surface smoothness and tensile strength.

Printing temperature has a major effect on the extrusion and bonding behavior of PLA. Higher temperatures (e. g., 210 0C) mean the polymer chains have more freedom of motion, which results in better inter, layer adhesion and higher mechanical strength. On the other hand, very high temperatures can lead to material degradation or poor dimensional stability.

Infill density determines how much material is used in the interior of a printed part. A 100% infill is a completely solid part that generally provides the highest strength and stiffness. Lower infill levels shorten the printing time and save material, but also weaken the part. Infill density has been identified as the single most affecting parameter to tensile properties. The three parameters were selected based on research findings and their practical use in PLA, based FDM printing. The values range allows for assessing the trade, off between mechanical performance, material consumption, and printing speed. The L9

Taguchi orthogonal array was chosen to efficiently explore the effect of each factor with only 9 experimental runs.

Specimens for tensile testing were printed in accordance with ASTM D638 Type V dimensions.

2.4. Mechanical Testing

Tensile properties were evaluated using a Universal Testing Machine (UTM, Model: Instron 3369, Instron Corporation, USA) with a 10 kN load cell in accordance with ASTM D638 Type V standard. The specimens were clamped with a grip length of 25 mm, and the test was conducted at a crosshead speed of 5 mm/min under ambient laboratory conditions. The obtained stress–strain data were used to determine the ultimate tensile strength, elongation at break, and Young’s modulus of the printed specimens.

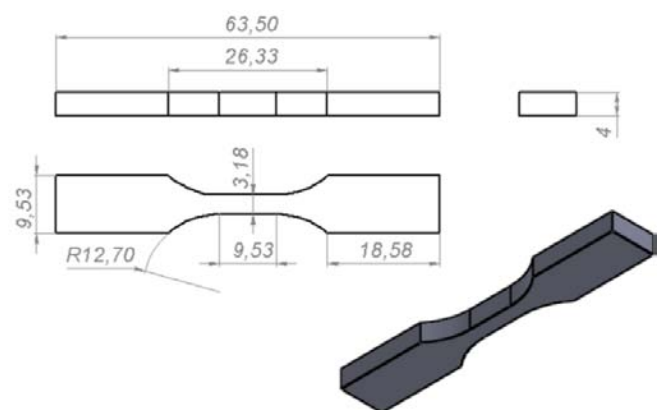


Figure 1: ASTM D638 Type V Tensile Specimen Dimension.

Dynamic mechanical analysis (DMA) was performed using a DMA Q800 (TA Instruments, USA) in tension mode over a temperature range of 25 °C to 120 °C, at a heating rate of 3 °C/min and frequency of 1 Hz. The measurements provided insights into the storage modulus (E'), loss modulus (E''), and damping behavior ($\tan \delta$) of the PLA/PBAT blend, enabling

evaluation of its viscoelastic and relaxation characteristics.

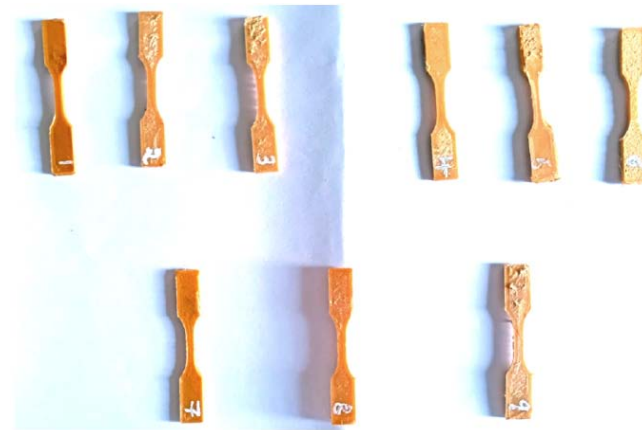


Figure 2: 3D Printed Specimens of PLA/PBAT/Joncryl.

2.5. Morphological Analysis

The morphological characteristics of the fractured tensile specimens were examined using Scanning Electron Microscopy (SEM) (Model: FEI Quanta 200, Thermo Fisher Scientific, USA) to evaluate phase dispersion, interfacial adhesion, and fracture mechanisms of the PLA/PBAT/Joncryl blends. Prior to imaging, the samples were sputter-coated with a thin layer of gold to minimize charging and improve image quality. SEM micrographs were captured at a magnification of 100 \times to observe the distribution of dispersed domains and fracture features.

3. RESULTS AND DISCUSSION

3.1. Tensile Testing

The mechanical performance of the PLA/PBAT/Joncryl 3D printed specimens, as influenced by the process parameters, is clearly reflected in the experimental results of the Taguchi L9 orthogonal array (Table 3). Trial 3, which featured a 0.16 mm layer

height, 210 C printing temperature, and 100% infill density, led to the highest ultimate tensile strength (UTS) of 41.20 N/mm and maximum elongation of 12.42%. Thus, the sample was not only structurally strong but also ductile, suggesting that the fine layer deposition, elevated thermal energy for fusion, and dense internal structure had a synergistic effect. On the other hand, a lowest UTS (28.79 N/mm) and low elongation (7.22%) were observed in the Trial 9, where a 0.24 mm layer height, 200 C, and 50% infill were used. The thick layers and lower internal density were, therefore, the most significant factors contributing to the mechanical integrity.

Each parameter was scrutinized separately; layer height seemed to play a mechanical performance inverse relationship. Situations with 0.16 mm layer height were always more successful than those with 0.24 mm, thereby confirming that thinner layers facilitate interlayer adhesion and reduce the formation of voids. Similarly, the printing temperature was positively correlated with UTS and elongation, with 210 C giving the best results. Increased temperatures enhance melt flow and inter, diffusion between layers, thus, strengthening the interfacial bonds. Infill density was the parameter that had the most significant effect; by increasing it from 50% to 100%, the strength and ductility were largely raised, as several trials have shown. Denser infill basically removes porosity and stress concentration sites, thus, the part can carry higher loads and deform more uniformly.

The best overall combination for mechanical performance, i. e., a 0.16 mm layer height, printing at 210 C, and 100% infill density, corresponds to the Trial 3 parameter set, thus confirming the results of the Taguchi S/N ratio analysis and physical testing. These findings highlight the significance of process optimization in FDM, particularly when using polymer blends such as PLA/PBAT/Joncryl. Adjusting parameters to obtain a fine resolution, adequate

Table 3: Experimental Results Showing the Effect of Layer Height (LH), Printing Temperature (PT), and Infill Density (ID) on the Ultimate Tensile Strength (UTS) and Percentage Elongation of FDM-Printed PLA Specimens

Trails	Layer Height - LH (mm)	Printing Temp -PT (°C)	Infill Density - ID (%)	UTS (N/mm ²)	SN Ratio	% Elongation
1	0.16	190	50	29.52	29.40	7.82
2	0.16	200	75	34.64	30.79	10.12
3	0.16	210	100	41.20	32.29	12.42
4	0.2	200	100	38.09	31.61	11.02
5	0.2	210	50	30.84	29.78	8.22
6	0.2	190	75	30.04	29.55	7.32
7	0.24	210	75	33.24	30.43	8.72
8	0.24	190	100	35.86	31.09	10.54
9	0.24	200	50	28.79	29.18	7.22

Table 4: ANOVA Results for the Effect of Layer Height (LH), Printing Temperature (PT), and Infill Density (ID) on UTS of FDM-Printed PLA Specimens

Source	DOF	Seq SS	Adj SS	Adj MS	F-value	P-value	Cont. %
LH	2	0.62247	0.62247	0.31123	9.12	0.099	6.73
PT	2	1.03422	1.03422	0.51711	15.16	0.062	11.18
ID	2	7.52513	7.52513	3.76256	110.28	0.009	81.35
Residual error	2	0.06824	0.06824	0.03412			
Total	8	9.25005					

thermal energy, and high internal density allows the structural performance of biodegradable 3D, printed components to be improved to a great extent. These findings have real potential in the fields of biomedicine, packaging, and eco, friendly applications where the combination of strength and sustainability is required.

An Analysis of Variance (ANOVA) (Table 4) was used to determine the contribution of each FDM process parameter Layer Height (LH), Printing Temperature (PT), and Infill Density (ID) to the Ultimate Tensile Strength (UTS) of PLA/PBAT/ Joncryl samples. Based on the three factors, Infill Density was the one that had the most dominant influence, contributing 81.35% of the total variance. The extremely high F, value (110.28) and a P, value of 0.009, which is well below the 0.05 threshold for statistical significance, confirm this finding. The 100% infill, thus, provides a mechanically strong structure through the complete removal of voids and an increase in load, bearing volume, which directly leads to tensile strength being enhanced.

Printing Temperature showed the second-highest influence on UTS, accounting for 11.18% of the total variation. The associated F, value (15.16) and P, value (0.062) show a moderately significant effect. The P, value is a bit higher than the standard 0.05 significance threshold, but the trend indicates that higher temperatures facilitate polymer flow and interlayer fusion, thus resulting in stronger parts. Layer Height, the least influential of the three, still accounted for 6.73% of the variation. With an F, value of 9.12 and a P, value of 0.099, its effect was less statistically significant but still relevant from a practical point of view, especially when combined with other optimized conditions.

The residual error was low (0.06824), showing that there was little unexplained variability and thus the reliability of the experimental design. In summary, the ANOVA results provide strong evidence that infill density is the most significant factor affecting the tensile strength of PLA/PBAT/Joncryl parts printed by FDM, followed by printing temperature and then layer

height. Only infill density is statistically significant ($P=0.009 < 0.05$). Printing temperature ($P=0.062$) and layer height ($P=0.099$) show non-significant trends within the tested range. The findings are in close agreement with the trends observed in the S/N ratio analysis and the raw experimental results, thus confirming the consistency of the Taguchi method in process parameter optimization for enhanced mechanical performance.

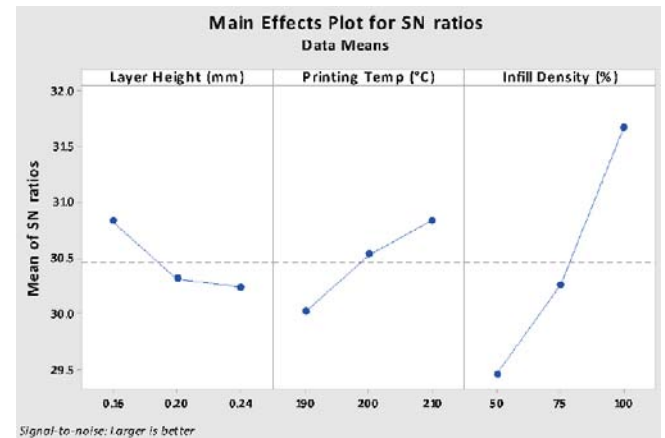


Figure 3: Main effects plot for signal-to-noise (S/N) ratios showing the influence of Layer Height (mm), Printing Temperature (°C), and Infill Density (%) on the mechanical performance of 3D-printed PLA/PBAT/Joncryl components.

The Main Effects Plot for SN Ratios (Figure 3) helps interpret the impact of each factor on the mean signal-to-noise (SN) ratio, with the goal of "larger is better".

The Taguchi, based signal, to, noise (S/N) ratio analysis conveys how the processing parameters individually interact with the mechanical behavior of the 3D, printed PLA/PBAT/Joncryl blend specimens. To enhance tensile performance, the "larger, the, better" criterion ensured a strong assessment in the presence of minor fluctuations in the experiments.

Layer height was a paramount factor in mechanical strength. The study found that thinner layers (0.16 mm in particular) were always associated with higher S/N ratios. This is due to a more accurate deposition profile that, as a result of higher surface area contact and more uniform cooling, stronger interlayer bonding is

achieved. Besides the layer thickness, internal voids and layer gaps, which are usual crack propagation sources under tensile load, also become less frequent. Although thinner layers lead to longer printing time, the mechanical trade-off is positive, especially for the fields of application that needs strength and structural precision.

The tensile performance improved with the printing temperature up to 210C. This behavior is consistent with the rheological properties of PLA and PBAT, as higher temperatures result in lower melt viscosity and thus allow better chain diffusion at the interface of the adjoining layers. Stronger weld lines and less delaminating are the outcomes of increased molecular entanglement at higher temperatures. On the other hand, it is advisable not to go beyond the thermal degradation point of PLA, which is around 230C, because discoloration, hydrolytic breakdown, and loss of mechanical integrity could occur. 210C was considered the best temperature within the ranged tested, as it balanced the flow characteristics with the thermal stability. The infill density was the factor that influenced the most the tensile performance among the three. The S/N ratio increased significantly with the infill from 50% to 100%. A denser infill structure not only provides continuous load pathways but also a greater volume of material to resist the deformation. Voids at low infill densities dominate the internal structure and thus act as stress concentrators which not only lower the strength but also the reproducibility of the samples. 100% infill essentially represents a solid cross, section and thus the anisotropy is almost completely eliminated and the dimensional stability which is of great

importance for structural parts and functional prototypes is enhanced.

Interestingly, the S/N trend analysis did not reveal any statistically significant adverse interaction effects between the selected factors, implying that their contributions to tensile strength are fairly independent within the chosen levels. Nevertheless, designers need to weigh these settings against other factors such as print time, material usage, and thermal warping. For instance, although 100% infill and 0.16 mm layer height enhance mechanical properties to the maximum, they also prolong printing time and increase material consumption considerably.

The Taguchi DoE method has successfully pinpointed a parameter set 0.16 mm layer, 210C, and 100% infill that achieves the maximum tensile strength with minimal process variation. These results serve as a scientific guide for parameter setting when fabricating biodegradable, mechanically strong PLA/PBAT/Joncryl 3D printed parts, especially in scenarios where strength, accuracy, and eco-friendliness co-exist.

The standardized residuals generally follow a straight line, which suggests that the residuals are approximately normally distributed (Figure 4). This supports the assumption of normality. The standardized residuals appear randomly scattered around zero with no clear pattern. This supports the assumption of constant variance (homoscedasticity) and suggests the model is appropriately fitted.

The histogram is roughly symmetric and centered around zero, though the sample size is small (only 9

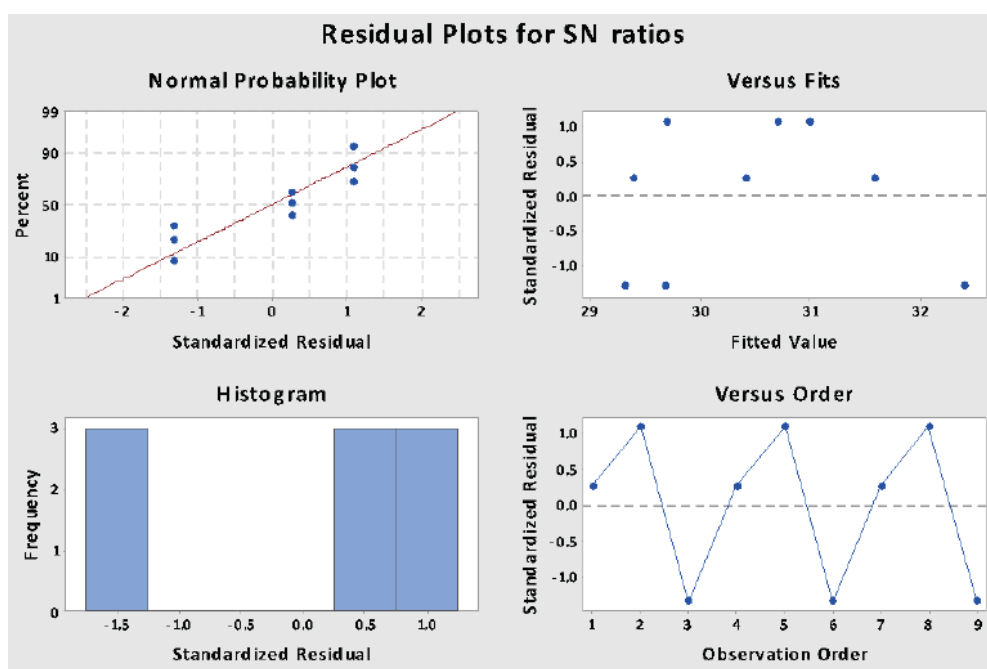


Figure 4: Residual plots for S/N ratios showing (a) normal probability, (b) residuals versus fits, (c) histogram of residuals, and (d) residuals versus observation order for the ANOVA model.

values), so it's coarse. Indicates that residuals are fairly normally distributed, with no extreme skewness or outliers. There's a slight zigzag pattern, but generally, the trend or drift is not noticeable over time. The time, based correlation or pattern is not significant, and it suggests that the observations are independent. The residual plots do not reveal any substantial breaches of regression assumptions, and therefore, the model is probably statistically valid for understanding SN ratios.

3.2. Surface Morphology of FDM-Printed PLA/PBAT/Joncryl Composites

The SEM images of PLA/PBAT composites at various infill densities (Figure 5) visually demonstrate how the internal structure affects the morphology and interfacial bonding of the printed samples. The surface at 100% infill is dense and compact with very few voids, thus showing strong interlayer adhesion and uniform material deposition, which in turn directly strengthens the mechanical performance and durability of the printed part. On the other hand, the 75% infill sample shows small voids and partial interlayer gaps, thus a decrease in bonding quality compared to the fully dense structure. Such an intermediate morphology reflects a trade-off between mechanical performance and material efficiency thus, it can be used in applications where moderate strength and reduced material usage are required. The 50% infill specimen

shows a highly porous structure with large voids and weak interlayer fusion, which will inevitably lead to the reduction of tensile and impact properties of the composite. It is true that such low infill densities reduce the weight and the printing costs; however, they also create stress concentration points that can cause premature failure under loading. The SEM analysis depicts that higher infill percentages result in better structural integrity and interfacial bonding, while lower infill densities increase porosity, thus, decreasing the overall mechanical performance of PLA/PBAT/ Joncryl composites.

3.3. Dynamic Mechanical Analysis (DMA) Testing

The Dynamic Mechanical Analysis (DMA) graph (Figure 6) illustrates the influence of infill density on the storage modulus (E') of PLA/PBAT blend samples as a function of temperature. The storage modulus is the measure of the material's elastic (or stiff) behavior in response to time-varying loads. At lower temperatures, the samples with 100% infill density display a greater than average storage modulus (approximately 2200 MPa) than all the other infill densities observed (75% and 50% infill's), which indicates that they have more stiffness due to their thicker properties and more capacity to carry a load [21-23]. The second highest storage modulus is displayed by the 75% infill density sample (approximately 1800 MPa) and the least

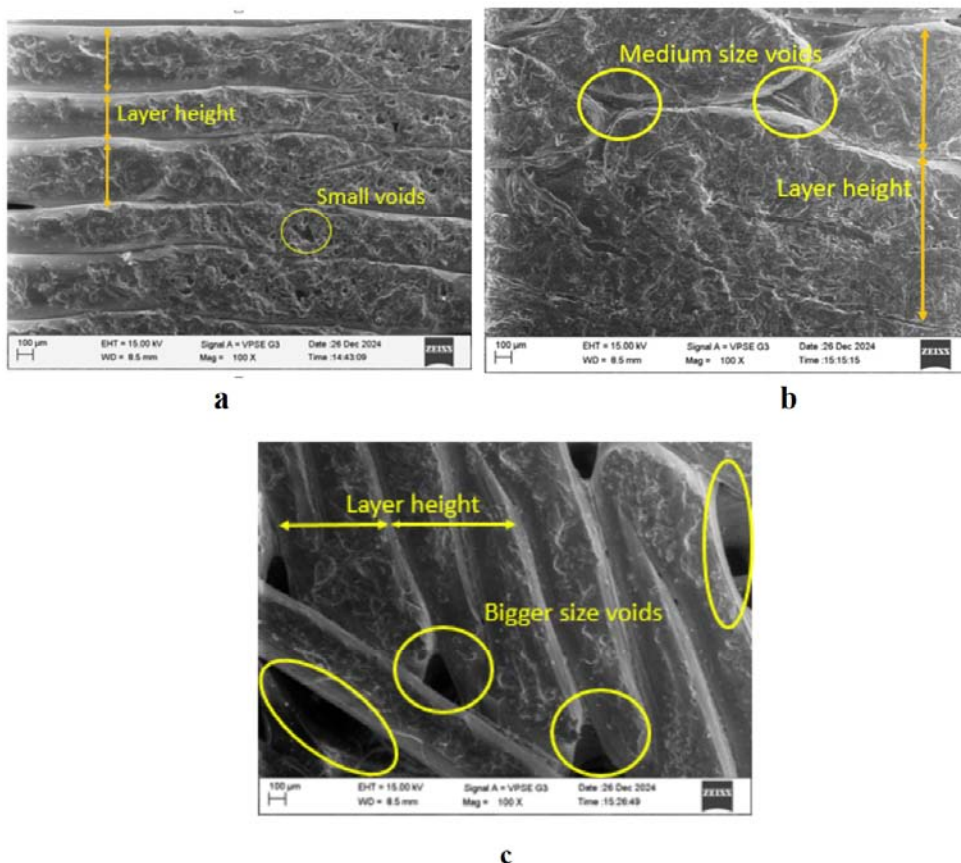


Figure 5-a,b,c: SEM image of tensile specimens with different infill density (a:100 %, b:75% and c:50%).

available to carry the load at all temperatures is the samples having the 50% fill (approximately 900 MPa). The modulus decreases due to a lower density and a corresponding increase in the total void volume, affecting the overall load-bearing capacity of that type of manufacturing.

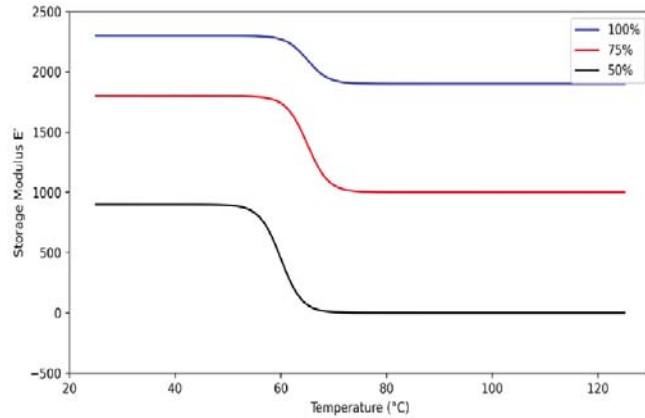


Figure 6: Dynamic Mechanical Analysis (DMA) curves showing the variation of Storage Modulus (E') with temperature for PLA/PBAT/ Joncryl blend samples with different infill densities (100%, 75%, and 50%).

Upon heating, all samples exhibit a marked decrease in storage modulus around 60-80°C, which is indicative of the glass transition temperature (T_g) of the PLA/PBAT blend. This change in the material is associated with the change of the glassy, rigid state to the rubbery, soft phase. The reduction of the modulus steeply almost twice as much for the lower infill density samples (50% and 75%), thus they are more vulnerable to thermal softening due to their higher amorphous content and the presence of structural voids. After T_g , the modulus remains at a lower level, with the 100% infill sample still having a higher residual stiffness than the 75% and 50% infill samples.

The DMA data for the most part show that the material becomes stiffer and thermally more resistant with the increase of the infill density. On the other hand, samples with lower infill densities show an increase of free volume and porosity, which results in a significant decrease in storage modulus and mechanical rigidity. This evidences that the infill density is the main factor determining the dynamic mechanical behavior of 3D, printed PLA/PBAT parts, especially in the case of use at higher temperatures where the maintenance of dimensions and the ability to carry a load are required.

This Tan Delta (δ) vs. Temperature graph (Figure 7) from DMA analysis represents the damping behavior of PLA/PBAT blend samples with varying infill densities (100%, 75%, and 50%). The tan delta peak indicates the glass transition temperature (T_g), where the polymer chains gain mobility, transitioning from a rigid glassy state to a more flexible rubbery state.

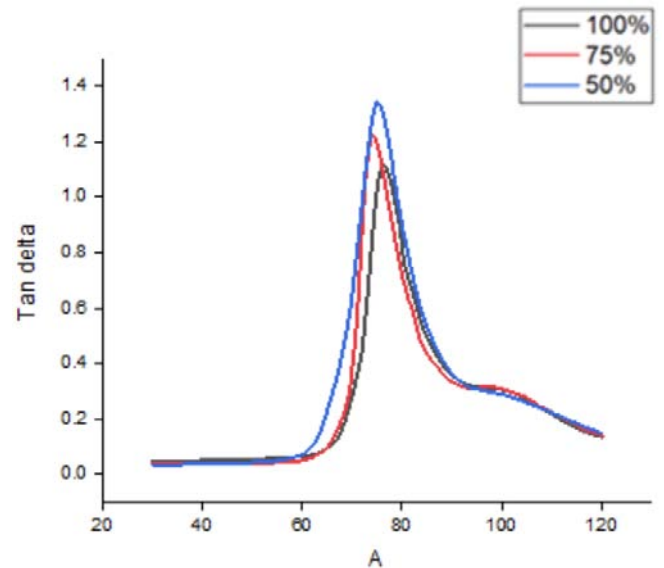


Figure 7: Tan Delta (δ) versus Temperature curves obtained from Dynamic Mechanical Analysis (DMA) of PLA/PBAT/ Joncryl blend samples with varying infill densities (100%, 75%, and 50%).

The 100% infill sample (black curve) displays the highest tan delta peak (~ 1.35) by a factor of more than 7 at around 75-80°C. This is indicative of maximum damping as well as energy dissipation. The larger peak represents a significant viscous response since the dense structure limits molecular motion and thus leads to higher internal friction at T_g . The 75% infill sample (red curve) has a peak slightly lower (~ 1.2) at approximately the same temperature, which is indicative of a balance between elastic and viscous behaviour with the damping being reduced marginally due to the increase in porosity. The 50% infill sample (blue curve) shows the lowest tan delta peak (~ 1.1), thus it is an indicator of reduction in the damping capacity. The porous nature makes it possible for the chains to move more easily which results in a lesser viscous response and lower internal friction. Also, the peak width increases as infill density decreases, meaning that lower infill structures have a more heterogeneous transition region due to the presence of more free volume and fewer chain entanglements.

4. CONCLUSION

The results of the mechanical, statistical, morphological, and dynamic analyses combine to tell a single, clear story that reveals the underlying connection between FDM process parameters and the final properties of the printed PLA/PBAT/ Joncryl components.

The exploration of data pivots on the statistical underpinning offered by the ANOVA figures, which singles out infill density as the factor that most decisively affects the tensile strength. The figure is as impressive as it is clear: 81.35% of the total variance

can be attributed to this single variable. Far from being a mere theoretical proposition, this result lays down a definite order of the variables to be controlled by engineers and designers. The supreme role of infill density is such that in any case where strength is a critical requirement; it should be the first parameter to be adjusted.

Furthermore, this statistical statement is substantiated in reality through the SEM images. The morphology of the fracture surfaces links the changes in infill directly to the changes in the internal structure. The improved microstructure is the main reason for the enhanced macro-scale properties, as confirmed through tensile testing and DMA. The 100% infill sample showed the highest UTS (41.20 N/mm²) and elongation (12.42%), mainly due to its dense and well-fused structure, which provides a larger effective load-bearing area and minimizes stress concentration by reducing porosity.

DMA results support this trend, where the same specimen exhibited the highest storage modulus, indicating greater stiffness and resistance to deformation under dynamic loading. The increased $\tan \delta$ peak further suggests a uniform structure with controlled polymer chain mobility, leading to improved thermo-mechanical stability. The process parameter (100% infill) results in a superior microstructure, which directly governs improved mechanical and thermal properties, forming a clear basis for process optimization in sustainable FDM manufacturing.

REFERENCES

- [1] Mobarak MH, Abid AS, Munna MS, Dutta M, Rimon MIH. Additive manufacturing in biomedical: Applications, challenges, and prospects. *Hybrid Advances* 2025; 10: 100467. <https://doi.org/10.1016/j.hybadv.2025.100467>
- [2] Gao W, Zhang Y, Ramanujan D, Ramani K, Chen Y, Williams CB, Wang CC, Shin YC, Zhang S, Zavattieri PD. The status, challenges, and future of additive manufacturing in engineering. *Computer-Aided Design* 2015; 69: 65-89. <https://doi.org/10.1016/j.cad.2015.04.001>
- [3] Kristiawan RB, Imaduddin F, Ariawan D, Ubaidillah, Arifin Z. A review on the fused deposition modeling (FDM) 3D printing: Filament processing, materials, and printing parameters. *Open Engineering* 2021; 11(1): 639-649. <https://doi.org/10.1515/eng-2021-0063>
- [4] Turner BN, Gold SA. A review of melt extrusion additive manufacturing processes: II. Materials, dimensional accuracy, and surface roughness. *Rapid Prototyping Journal* 2015; 21(3): 250-261. <https://doi.org/10.1108/RPJ-02-2013-0017>
- [5] Samir A, Ashour FH, Hakim AA, Bassyouni M. Recent advances in biodegradable polymers for sustainable applications. *Npj Materials Degradation* 2022; 6(1): 68. <https://doi.org/10.1038/s41529-022-00277-7>
- [6] Auras RA, Lim LT, Selke SE, Tsuji H, Eds. *Poly (lactic acid): synthesis, structures, properties, processing, applications, and end of life*. John Wiley & Sons 2022. <https://doi.org/10.1002/9781119767480>
- [7] Farah S, Anderson DG, Langer R. Physical and mechanical properties of PLA, and their functions in widespread applications—A comprehensive review. *Advanced Drug Delivery Reviews* 2016; 107: 367-392. <https://doi.org/10.1016/j.addr.2016.06.012>
- [8] Taubner M, Shishoo R. Influence of processing parameters on the degradation of PLA during extrusion. *Polymer Degradation and Stability* 1998; 59(1-3): 213-220.
- [9] Taghinezhad SF, Mansourieh M, Abbasi A, Major I, Pezzoli R. Improved compatibilized TPS/PLA blends: effects of singular and binary compatibilization systems. *Carbohydrate Polymer Technologies and Applications* 2025; p. 100819. <https://doi.org/10.1016/j.carpta.2025.100819>
- [10] Taleb K, Saidi-Besbes S, Pillin I, Grohens Y. Biodegradable poly (butylene succinate) nanocomposites based on dimeric surfactant organomodified clays with enhanced water vapor barrier and mechanical properties. *ACS Omega* 2022; 7(47): 43254-43264. <https://doi.org/10.1021/acsomega.2c05964>
- [11] Shen Y, Jin B, Ren L, Gan H, Li J, Zhao D, Shen H, Zhang M. Fully Biodegradable Poly (lactic acid)/Poly (butylene adipate-co-terephthalate) Blends with highly toughness Based on in situ Interfacial Compatibilization by functional epoxy compound 2025. <https://doi.org/10.21203/rs.3.rs-6564026/v1>
- [12] Wang D, Li Y, Xie XM, Guo BH. Compatibilization and morphology development of immiscible ternary polymer blends. *Polymer* 2011; 52(1): 191-200. <https://doi.org/10.1016/j.polymer.2010.11.019>
- [13] He H, Wang G, Chen M, Xiong C, Li Y, Tong Y. Effect of different compatibilizers on the properties of poly (lactic acid)/poly (butylene adipate-co-terephthalate) blends prepared under intense shear flow field. *Materials* 2020; 13(9): 2094. <https://doi.org/10.3390/ma13092094>
- [14] Lendvai L, Brenn D. Mechanical, morphological and thermal characterization of compatibilized poly (lactic acid)/thermoplastic starch blends. *Acta Technica Jaurinensis* 2020; 13(1): 1-13. <https://doi.org/10.14513/actatechjaur.v13.n1.532>
- [15] Oguz H, Dogan C, Kara D, Ozen ZT, Ovali D, Nofar M. Development of PLA-PBAT and PLA-PBSA bio-blends: Effects of processing type and PLA crystallinity on morphology and mechanical properties. In *AIP Conference Proceedings*. AIP Publishing LLC 2019; 2055(1): 030003. <https://doi.org/10.1063/1.5084813>
- [16] Ning F, Cong W, Qiu J, Wei J, Wang S. Additive manufacturing of carbon fiber reinforced thermoplastic composites using fused deposition modeling. *Composites Part B: Engineering* 2015; 80: 369-378. <https://doi.org/10.1016/j.compositesb.2015.06.013>
- [17] Gonzalez YE, Mendoza JM, Durán JR, Vertel LCT, Rhenals-Julio JD. Effect of printing parameters on mechanical properties and processing time of additively manufactured parts. *Matéria (Rio de Janeiro)* 2023; 28: e20230111. <https://doi.org/10.1590/1517-7076-rmat-2023-0111>
- [18] Popescu D, Zapciu A, Amza C, Baci F, Marinescu R. FDM process parameters influence over the mechanical properties of polymer specimens: A review. *Polymer Testing* 2018; 69: 157-166. <https://doi.org/10.1016/j.polymertesting.2018.05.020>
- [19] Zolfagharian A, Khosravani MR, Kaynak A. Fracture resistance analysis of 3D-printed polymers. *Polymers* 2020; 12(2): 302. <https://doi.org/10.3390/polym12020302>
- [20] Bhiogade A, Kannan M. Studies on thermal and degradation kinetics of cellulose micro/nanoparticle filled polylactic acid (PLA) based nanocomposites. *Polymers and Polymer Composites* 2021; 29(9 suppl): S85-S98. <https://doi.org/10.1177/0967391120987170>
- [21] Gonabadi H, Yadav A, Bull SJ. The effect of processing parameters on the mechanical characteristics of PLA produced by a 3D FFF printer. *The International Journal of Advanced Manufacturing Technology* 2020; 111: 695-709. <https://doi.org/10.1007/s00170-020-06138-4>

- [22] Müller M, Valášek J, Šleger M. Effect of infill density in FDM 3D printing on low-cycle fatigue behavior of PLA materials. *Polymers* 2022; 14(22): 4930. <https://doi.org/10.3390/polym14224930>
- [23] Turaka S, Prasad ASG, Reddy AK, Naidu MT. Impact of infill density on morphology and mechanical performance of MEX/FFF manufactured polymer composite components *Heliyon* 2024; 10. <https://doi.org/10.1016/j.heliyon.2024.e29920>

Received on 22-12-2025

Accepted on 20-01-2026

Published on 04-02-2026

<https://doi.org/10.6000/1929-5995.2026.15.03>

© 2026 Raju *et al.*

This is an open-access article licensed under the terms of the Creative Commons Attribution License (<http://creativecommons.org/licenses/by/4.0/>), which permits unrestricted use, distribution, and reproduction in any medium, provided the work is properly cited.